International Journal of Mass Spectrometry 435 (2019) 114–117

Contents lists available at ScienceDirect

International Journal of Mass Spectrometry

journal homepage: www.elsevier.com/locate/ijms

Short communication

Activation of hydroxylamine by single gold atomic anions☆

Gaoxiang Liu, Sandra M. Ciborowski, Zhaoguo Zhu, Kit H. Bowen*

Department of Chemistry, Johns Hopkins University, 3400 N. Charles Street, Baltimore, MD 21218, USA

ARTICLE INFO

Article history:
Received 17 June 2018
Received in revised form 9 October 2018
Accepted 11 October 2018
Available online 21 October 2018

Keywords:
Anion photoelectron spectroscopy
Single atom molecular activation

ABSTRACT

Hydroxylamine (HA) is a potential component in next-generation monopropellants. In this work, we present a combined anion photoelectron spectroscopic and density functional theory study of the reaction between a single HA molecule and a single gold atomic anion, Au^-. This study shows that an Au- anion can activate a HA molecule by inserting into its N–O bond. Our calculations show this reaction to be facilitated by the presence of two minimum energy crossing points (MECP's), i.e., spin flips, along the reaction pathway.

1. Introduction

Replacing hydrazine with less toxic ionic liquids as monopropellants in spacecraft thrusters is appealing from both a safety and an environmental perspective. Hydroxylammonium nitrate (HAN) is one such ionic liquid being considered. In fact, HAN is a component in the monopropellant used in NASA's Green Propellant Infusion Mission [1,2]. Studies of both the thermal and catalytic decomposition mechanisms of HAN have informed the further development of HAN-based monopropellants and thus of thrusters [3–18]. Hydroxylamine (H_2NOH, HA) is a major thermal decomposition product of HAN. As such, HA can further decompose on heated iridium catalysts, creating ignition conditions in HAN-based propellants [17,19].

Single metal atoms are sometimes seen as models for mimicking active sites in heterogenous catalysts [20–25]. Studying molecular activation and catalysis using gas-phase, metal atomic ions can help to better understand bond activation, dissociation, and new bond formation at the molecular level and thus to aid the design of new catalysts [26–29]. In the present work, we focused on studying the activation of HA by single gold atomic anions. Molecular activation by gold ions has received considerable attention in gas-phase studies. While the gold atomic cation has been found to activate various molecules [30–34], the gold atomic anion tends to be inert in activating small molecules [35–42]. An exception, however, is the activation of CO_2 by Au^-, a process that involves only charge transfer and not bond breaking [43,44]. Here, we utilize a combination of anion photoelectron spectroscopy and density functional theory (DFT) to provide strong evidence that Au- can break the N–O bond in HA, thus activating it. As shown below, Au- spin states play critical roles in activating HA.

2. Experimental and computational methods

Anion photoelectron spectroscopy is conducted by crossing a beam of mass-selected negative ions with a fixed-frequency photon beam and energy-analyzing the resultant photodetached electrons. The photodetachment process is governed by the energy-conserving relationship: $h\nu = EBE + EKE$, where $h\nu$ is the photon energy, EBE is the electron binding energy, and EKE is the electron kinetic energy. Our apparatus consists of a laser vaporization cluster anion source with an attached ligation cell, a time-of-flight mass spectrometer, a Nd:YAG photodetachment laser (operating at 355 nm), and a magnetic bottle electron energy analyzer with a resolution is ~35 meV at 1 eV EKE [45]. Photoelectron spectra were calibrated against the well-known atomic transitions of atomic Cu^- [46].

The interaction between Au^- and HA was studied using a laser vaporization-reaction cell arrangement [47]. Atomic gold anions were generated by laser vaporization of a pure gold foil wrapped around an aluminum rod. The resultant plasma was cooled with helium gas delivered by a pulsed valve, having a backing pressure of 100 psig. The resulting gold anions then traveled through a ligation cell (4-mm diameter), where it encountered HA/H_2O mixed vapor. The HA/H_2O mixed vapor was introduced into the ligation cell by a second pulsed valve, within which resided a drop of hydroxylamine water solution (Since HA in its pure form is hazardous, it is sold dissolved in water, 50 wt%). The resulting $[Au(HA)]^-$ anionic clusters

☆ Helmut Schwarz Honour Issue.

* Corresponding author.
E-mail address: kbowen@jhu.edu (K.H. Bowen).

https://doi.org/10.1016/j.ijms.2018.10.020
1387-3806/

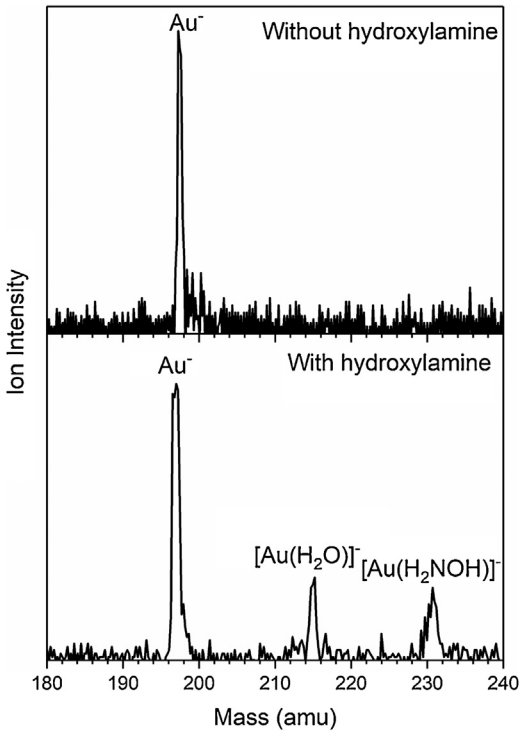

Fig. 1. The mass spectra of Au^- anions without and with the addition of HA/H_2O mixed vapor.

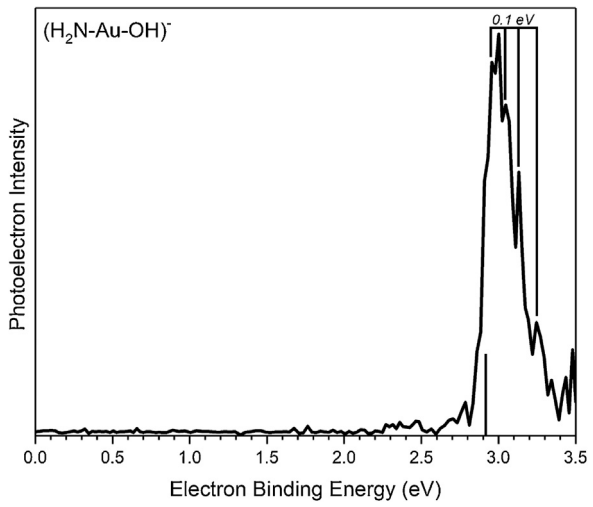

Fig. 2. The photoelectron spectrum of $[Au(HA)]^-$ taken by 3rd harmonic output of a Nd:YAG laser (3.496 eV). The stick spectrum represents the calculated VDE value.

were then mass-analyzed and mass-selected by the time-of-flight mass spectrometer and their photoelectron spectra measured.

Density functional theory calculations were performed with the ORCA computational chemistry software package [48]. All calculations were carried out with the PBE0 functional [49,50] with the D3 dispersion correction [51] and the RIJCOSX approximation [52]. The Ahlrichs Def2 basis sets, Def2-TZVP were used throughout our calculations [53]. The Stuttgart effective core potential, SDD [54] and the ECP basis set, Def2-TZVP|Def2-TZVP/J were used for the gold atoms. Vertical detachment energies (VDE) were computed from the energetic difference between the relaxed anionic complex and its corresponding neutral species at the geometry of the relaxed anion. Frequency calculations were performed to verify that no imaginary frequencies existed and all optimized structures were minima. The minimum-energy crossing points (MECPs) for the intersection of the electronic states of different spin multiplicities were searched for and located by using the method developed by Harvey et al. [55].

3. Results and discussions

The mass spectra with or without the addition of the HA/H_2O mixed vapor into the reaction cell are shown in Fig. 1. With no HA/H_2O mixed vapor, only Au^- was observed in the mass spectrum. After adding HA/H_2O vapor to the reaction cell, peaks due to both $[Au(H_2O)]^-$ and $[Au(HA)]^-$ complexes appeared in the mass spectrum, these resulting from the interaction of Au^- with HA or H_2O, respectively. $[Au(H_2O)]^-$ has been studied in our previous work and is not the focus of the current study [41]. $[Au(HA)]^-$, on the other hand, could exist either as $Au^-(HA)$, where HA is physisorbed onto Au^- or as a $[Au(HA)]^-$ complex, where one or more bonds in HA (N—H, O—H or N—O bond) have been broken. This latter case would correspond to the activation of HA.

To distinguish between these isomers, the anion photoelectron spectrum of $[Au(HA)]^-$ was measured. Typically, when an atomic metal anion is physisorbed by another molecule, the photoelectron spectrum of the resulting weakly-attached cluster anion closely resembles that of the atomic anion alone, since that anion acts as the chromophore. Thus, except for being shifted to higher electron binding energy (EBE) and its features slightly broadened, the resulting photoelectron spectrum looks like that of the atomic anion. Fig. 2 presents the anion photoelectron spectrum of [Au(HA)]-. The evident feature in this spectrum reaches its maximal intensity at EBE = 3.00 eV. Thus, 3.00 eV is determined as the vertical detachment energy (VDE) value, i.e., the transition energy at which the Franck-Condon overlap between the anion's wavefunction and that of its neutral counterpart is at its maximum. Vibrational progressions spaced by 0.1 eV are also observed. The EBE of Au- alone would have been at 2.3 eV, i.e., its electron affinity. Since the observed difference between the VDE values of Au- and [Au(HA)]- is, at ~0.7 eV, relatively large for an ion-molecule interaction energy, and since there is evident vibrational excitation in the spectrum, it is clear that this is not the spectrum of the anion-molecule physisorbed complex, Au-(HA). The observed spectrum implies that a strong chemical interaction has occurred between Au- and HA, indicating hydroxylamine has been activated by its interaction with Au-.

Fig. 3 presents the DFT optimized structures of different $[Au(HA)]^-$ isomers. The global minimum of $[Au(HA)]^-$ has structure in which the Au^- inserts into the N–O bond of HA, that is, H_2N-Au–OH^-. The other isomers, H_2NO-Au-H^-, H-Au-$NHOH^-$ and $Au^-(H_2NOH)$ are essentially iso-energetic, although all of them are ~1.8–1.9 eV higher than the global minimum. The VDE of the global minimum H_2N-Au–OH^- is calculated to be 2.91 eV, which agrees well with the experimental VDE of 3.00 eV. Because H_2N-Au–OH^- is the most stable calculated isomer and since its calculated VDE agrees with the experimental value, we are confident that Au^- has inserted into the N–O bond of HA. The vibrational progression spaced at 0.1 eV is due to the bending modes of both N—H and O—H bonds.

The mechanism of HA activation by Au^- was investigated by DFT calculations. The resulting reaction pathway is presented in Fig. 4. The most salient feature of this pathway is the role of spin states. There, the singlet reactant, Au- is converted to a triplet transition state before being converted back to the singlet product. Initially, Au^- and HA are both in their singlet ground states. After having formed the singlet adduct, Au-(HA), in which HA is physisorbed to Au-, the insertion of Au- into the N–O bond begins to take place. Because of the rather high activation barrier (1.95 eV), however, the continuation of the reaction coordinate along the singlet surface is significantly hampered. Instead, the reaction can proceed

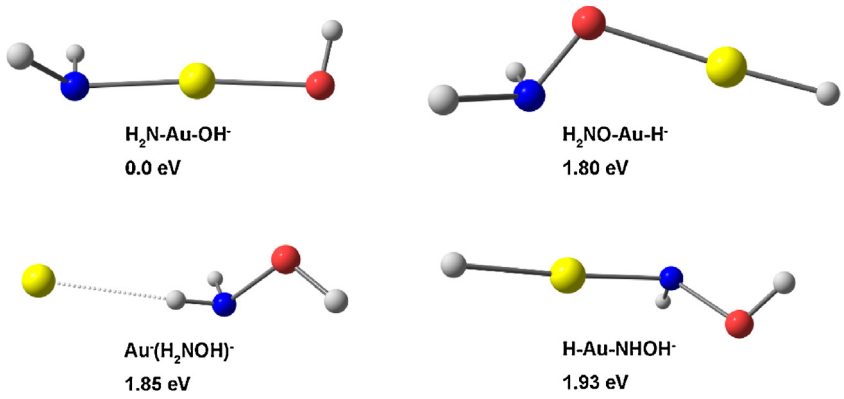

Fig. 3. Optimized structures for $[Au(HA)]^-$ and their relative energies.

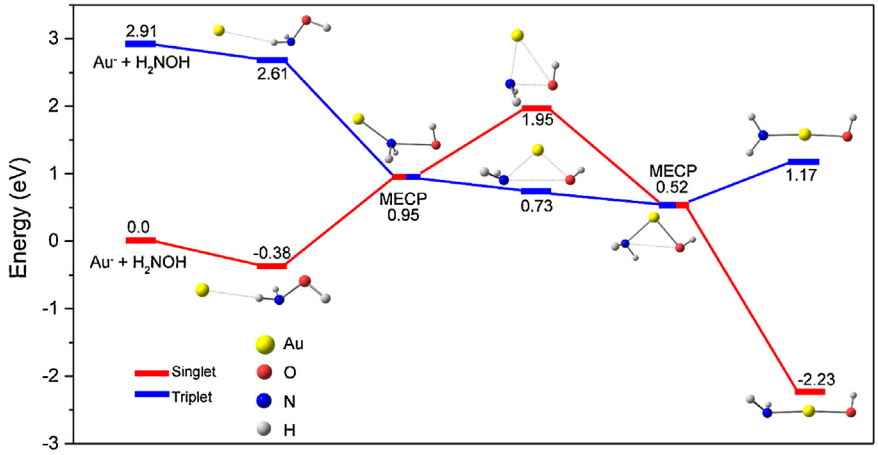

Fig. 4. Calculated reaction pathway for HA activation by Au^-. The numbers denote the relative energies of different structures.

more easily along the triplet transition state, which is only 0.73 eV above the entrance channel and much lower than the singlet transition state. The first minimal energy crossing point (MECP) is located between the physisorbed adduct and the transition states, where a crossover from the singlet to triplet surfaces occurs. This MECP is 0.95 eV higher than the entrance channel and 0.22 eV higher than the triplet transition state. Therefore, the highest barrier the reactants need to overcome is the first MECP rather than the triplet transition state. Once the first spin flip has occurred, the insertion of Au- into the N—O bond is essentially barrier-free. After passing through the triplet transition state, where the N—O bond is significantly lengthened, the activation complex encounters a second MECP, which converts it back to singlet state and to the final H_2N-Au-OH- product.

Usually gold anions are inert to the activation of molecules. Such inertness can be explained by its $d^{10}s^2$ ground state electron configuration: when a σ-bond is to be activated, the activating agent needs to have unpaired electrons, so that it can accept electrons from the bond to be activated. However, due to the lack of unpaired electrons in ground state Au^-, such electron transfer from the σ-bond to Au- is prohibited. An atomic orbital hybridization, which usually includes electron promotion to the 6p orbital, is thus required. According to our TDDFT calculations, the energy needed for such promotion is around 2.9 eV, which is too high to surmount. In the present case, however, the interaction of Au^- with HA can reduce this promotion energy from 2.9 eV to 0.95 eV. As shown in Fig. 4, at the first MECP the $[Au(HA)]^-$ complex converts from its singlet state to its triplet state, suggesting the creation of two unpaired electrons and empty orbitals on Au moiety which can then accept the two σ electrons of the N—O bond.

In summary, we have demonstrated that a single gold atomic anion can activate a hydroxylamine molecule by breaking its N—O bond, inserting there, and forming the H_2N-Au−OH^- complex. DFT calculations show that the spin crossover between singlet and triplet surfaces is critical for this activation to occur, as it creates the unpaired electrons and empty orbitals needed to accept the σ electron pair from the N—O bond.

Conflicts of interest

The authors declare no competing financial interest.

Acknowledgement

This material is based on work supported by the Air Force Office of Scientific Research (AFOSR) and the National Science Foundation (NSF) under grant numbers, FA9550-15-1-0259 and CHE-1664182, respectively. We are also grateful for valuable discussions with Dr. Stefan Schneider, Dr. Steve Chambreau, Dr. Jerry Boatz, and Dr. Ghanshyam Vaghjian at Edwards Air Force Base, CA.

References

[1] R. Amrousse, T. Katsumi, N. Azuma, K. Hori, Hydroxylammonium nitrate (HAN)-based green propellant as alternative energy resource for potential hydrazine substitution: from lab scale to pilot plant scale-up, Combust. Flame 176 (2017) 334–348.
[2] NASA GPIM. https://www.nasa.gov/mission_pages/tdm/ green/overview.html (accessed January 12, 2017).
[3] J.T. Cronin, T.B. Brill, Thermal decomposition of energetic materials. 8. Evidence of an oscillating process during the high-rate thermolysis of

hydroxylammonium nitrate, and comments on the interionic interactions, J. Phys. Chem. 90 (1986) 178–181.
[4] T.B. Brill, T.P. Russell, Rapid-scan infrared/thermal profiling studies of the thermal decomposition of selected nitrate salts of interest for emulsified propellants, Proc. SPIE (1988) 40–43.
[5] J.T. Cronin, T.B. Brill, Thermal decomposition of energetic materials 29. The fast thermal decomposition characteristics of a multicomponent material: liquid gun propellant 1845, Combust. Flame 74 (1988) 81–89.
[6] T.B. n, P.D. Spohn, J.T. Cronin, Thermal decomposition of energetic materials 32. On the instantaneous molecular nature of aqueous liquid gun propellants at high temperature and pressure before thermal decomposition, J. Energy Mech. Mater. Manuf. Eng. 8 (1990) 75–84.
[7] J.W. Schoppelrei, T.B. Brill, Spectroscopy of hydrothermal reactions 7. Kinetics of aqueous $[NH_3OH]NO_3$ at 463-523 K and 27.5 MPa by infrared spectroscopy, J. Phys. Chem. A 101 (1997) 8593–8596.
[8] Y.J. Lee, T.A. Litzinger, Combustion chemistry of HAN, TEAN, and XM46, Combust. Sci. Technol. 141 (1999) 19–36.
[9] H. Lee, T.A. Litzinger, Thermal decomposition of HAN-based liquid propellants, Combust. Flame 127 (2001) 2205–2222.
[10] H. Lee, T.A. Litzinger, Chemical kinetic study of HAN decomposition, Combust. Flame 135 (2003) 151–169.
[11] C. Kappenstein, L. Courtheoux, R. Eloirdi, S. Rossignol, D. Duprez, N. Pillet, Catalytic decomposition of han−water binary mixtures, 38th AIAA/ASME/SAE/ASEE Joint Propulsion Conference & Exhibit, Joint Propulsion Conferences (2002).
[12] L. Courtheoux, D. Amariei, S. Rossignol, C. Kappenstein, Thermal and catalytic decomposition of HNF and HAN liquid ionic as propellants, Appl. Catal. B 62 (62) (2006) 217–225.
[13] D. Amariei, L. Courtheoux, S. Rossignol, C. Kappenstein, Catalytic and thermal decomposition of ionic liquid monopropellants using a dynamic reactor: comparison of powder and sphere-shaped catalysts, Chem. Eng. Process. 46 (2007) 165–174.
[14] S. Banerjee, S.A. Shetty, M.N. Gowrav, C. Oommen, A. Bhattacharya, Adsorption and decomposition of monopropellant molecule HAN on Pd(100) and Ir(100) surfaces: a DFT study, Surf. Sci. 653 (2016) 1–10.
[15] C. Oommen, S. Rajaraman, R.A. Chandru, R. Rajeev, Catalytic decomposition of hydroxylammonium nitrate monopropellant, IPCBEE 10 (2011) 205–209.
[16] R. Amrousse, K. Hori, W. Fetimi, K. Farhat, HAN and ADN as liquid ionic monopropellants: thermal and catalytic decomposition processes, Appl. Catal. B 127 (2012) 121–128.
[17] R. Amrousse, T. Katsumi, N. Itouyama, N. Azuma, H. Kagawa, K. Hatai, H. Ikeda, K. Hori, New HAN-based mixtures for reaction control system and low toxic spacecraft propulsion subsystem: thermal decomposition and possible thruster applications, Combust. Flame 162 (2015) 2686–2692.
[18] R. Amrousse, T. Katsumi, Y. Niboshi, N. Azuma, A. Bachar, K. Hori, Performance and deactivation of Ir-based catalyst during hydroxylammonium nitrate catalytic decomposition, Appl. Catal. A Gen. 452 (2013) 64–68.
[19] S.D. Chambreau, D.M. Popolan-Vaida, G.L. VaghjianiY, S.R. Leone, Catalytic decomposition of hydroxylammonium nitrate ionic liquid: enhancement of NO formation, J. Phys. Chem. Lett. 8 (2017) 2126–2130.
[20] H. Schwarz, P. Gonzalez-Navarrete, J. Li, M. Schlangen, X. Sun, T. Weiske, S. Zhou, Unexpected mechanistic variants in the thermal gas-phase activation of methane, Organometallics 36 (2017) 8–17.
[21] S.M. Lang, T.M. Bernhardt, V. Chernyy, J.M. Bakker, R.N. Barnett, U. Landman, Selective C-H bond cleavage in methane by small gold clusters, Angew. Chem. Int. Ed. 56 (2017) 13406–13410.
[22] X.L. Ding, X.N. Wu, Y.X. Zhao, S.G. He, C–H bond activation by oxygen-centered radicals over atomic clusters, Acc. Chem. Res. 45 (2012) 382–390.
[23] H. Schwarz, How and why do cluster size, charge state, and ligands affect the course of metal-mediated gas-phase activation of methane? Isr. J. Chem. 54 (2014) 1413–1431.
[24] Z. Luo, A.W. Castleman Jr., S.N. Khanna, Reactivity of metal clusters, Chem. Rev. 116 (116) (2016) 14456–14492.
[25] D.K. Bohme, H. Schwarz, Gas-phase catalysis by atomic and cluster metal ions: the ultimate single-site catalysts, Angew. Chem. Int. Ed. 44 (2005) 2336–2354.
[26] H. Schwarz, S. Shaik, J. Li, Electronic effects on room-temperature, gas-phase C-H bond activations by cluster oxides and metal carbides: the methane challenge, J. Am. Chem. Soc. 139 (2017) 17201–17212.
[27] X.N. Li, X.P. Zou, S.G. He, Metal-mediated catalysis in the gas phase: a review, Chinese J. Catal. 38 (2017) 1515–1527.
[28] S. Zhou, J. Li, M. Schlangen, H. Schwarz, Bond activation by metal–carbene complexes in the gas phase, Acc. Chem. Res. 49 (2016) 494–502.
[29] J. Roithova, D. Schröder, Selective activation of alkanes by gas-phase metal ions, Chem. Rev. 110 (2010) 1170–1211.
[30] T.M. Bernhardt, Gas-phase kinetics and catalytic reactions of small silver and gold clusters, Int. J. Mass Spec. 243 (2005) 1–29.
[31] J.M. Weber, Gas Phase Chemistry of Gold Organogold Compounds, PATAI'S Chemistry of Functional Groups, 2014.
[32] S. Zhou, J. Li, X.N. Wu, M. Schlangen, H. Schwarz, Efficient room-temperature, Au^+-mediated coupling of a carbene ligand with methane to generate C_2H_x (x=4, 6), Angew. Chem. Int. Ed. 55 (2016) 441–444.
[33] C. Geng, J. Li, T. Weiske, M. Schlangen, S. Shaik, H. Schwarz, Electrostatic and charge-induced methane activation by a concerted double C–H bond insertion, J. Am. Chem. Soc. 139 (2017) 1684–1689.
[34] J. Li, S. Zhou, M. Schlangen, T. Weiske, H. Schwarz, On the origin of room-temperature, Au^+-mediated coupling of a methylene ligand with H_2: implications for the mechanism of methane dehydrogenation, Chem. Select 3 (2016) 444–447.
[35] A.P. Woodham, G. Meijer, A. Fielick, Activation of molecular oxygen by anionic gold clusters, Angew. Chem. Int. Ed. 51 (2012) 4444–4447.
[36] R. Pal, L.M. Wang, Y. Pei, L.S. Wang, X.C. Zeng, Unraveling the mechanisms of O_2 activation by size-selected gold clusters: transition from Superoxo to Peroxo Chemisorption, J. Am. Chem. Soc. 134 (2012) 9438–9445.
[37] R.F. Hockendorf, Y. Cao, M.K. Beyer, Gas-phase ion chemistry of small gold cluster anions, Organometallics 29 (2010) 3001–3006.
[38] W. Huang, H.J. Zhai, L.S. Wang, Probing the interactions of O_2 with small gold cluster anions (Au_n^-, n=1-7): chemisorption vs physisorption, J. Am. Chem. Soc. 132 (2010) 4344–4351.
[39] Y. Gao, W. Huang, J. Woodford, L.S. Wang, X.C. Zeng, Detecting weak interactions between Au^- and gas molecules: a photoelectron spectroscopic and Ab initio study, J. Am. Chem. Soc. 131 (2009) 9484–9485.
[40] H.J. Zhai, C. Burgel, V. Bonacic-Koutecky, L.S. Wang, Probing the electronic structure and chemical bonding of gold oxides and sulfides in AuO_n^- and AuS_n^- (n=1, 2), J. Am. Chem. Soc. 130 (2008) 9156–9167.
[41] W. Zheng, X. Li, S. Eustis, A. Grubisic, O. Thomas, H. de Clercq, K. Bowen, Anion photoelectron spectroscopy of Au-$(H_2O)_{1,2}$, $Au_2^-(D_2O)_{1\text{-}4}$, and $AuOH^-$, Chem. Phys. Lett. 444 (2007) 232–236.
[42] Y. Gao, X.C. Zeng, Water-promoted O_2 dissociation on small-sized anionic gold clusters, ACS Catal. 2 (2012) 2614–2621.
[43] X. Zhang, E. Lim, S.K. Kim, K.H. Bowen, Photoelectron spectroscopic and computational study of $(M\text{-}CO_2)^-$ anions, M = Cu, Ag, Au, J. Chem. Phys. 143 (2015), 174305.
[44] B.J. Knurr, J.M. Weber, Solvent-driven reductive activation of carbon dioxide by gold anions, J. Am. Chem. Soc. 134 (2012) 18804–18808.
[45] X. Zhang, G. Liu, G. Ganteför, K.H. Bowen, A.N. Alexandrova, PtZnH5-, A σ-aromatic cluster, J. Phys. Chem. Lett. 5 (2014) 1596–1601.
[46] J. Ho, K.M. Ervin, W.C. Lineberger, Photoelectron spectroscopy of metal cluster anions: Cu_n^-, Ag_n^-, and Au_n^-, J. Chem. Phys. 93 (1990) 6987–7002.
[47] G. Liu, S. Ciborowski, K. Bowen, Photoelectron spectroscopic and computational study of pyridine-ligated gold cluster anions, J. Phys. Chem. A 121 (2017) 5817–5822.
[48] F. Neese, The ORCA program system, WIREs Comput. Mol. Sci. 2 (2012) 73–78.
[49] J.P. Perdew, M. Ernzerhof, K. Burke, Rationale for mixing exact exchange with density functional approximations, J. Chem. Phys. 105 (1996) 9982–9985.
[50] J.P. Perdew, K. Burke, M. Ernzerhof, Generalized gradient approximation made simple, Phys. Rev. Lett. 77 (1996) 3865–3868.
[51] S. Grimme, J. Antony, S. Ehrlich, H. Krieg, A consistent and accurate ab initio parametrization of density functional dispersion correction (DFT-D) for the 94 elements H-Pu, J. Chem. Phys. 132 (2010), http://dx.doi.org/10.1063/1.3382344.
[52] F. Neese, F. Wennmohs, A. Hansen, U. Becker, Efficient, approximate and parallel hartree-fock and hybrid DFT calculations. A 'Chain-of-Spheres' algorithm for the hartree-fock exchange, Chem. Phys. 356 (2008) 98–109.
[53] F. Weigend, R. Ahlrichs, Balanced basis sets of Split Valence, triple zeta valence and quadruple zeta valence quality for H to Rn: design and assessment of accurac, Phys. Chem. Chem. Phys. 7 (2005) 3297–3305.
[54] D. Andrae, U. Häußermann, M. Dolg, H. Stoll, H. Preuß, Energy-adjusted ab initio pseudopotentials for the second and third row transition elements, Theor. Chim. Acta 77 (1990) 123–141.
[55] J.N. Harvey, M. Aschi, H. Schwarz, W. Koch, The singlet and triplet states of phenyl cation. A hybrid approach for locating minimum energy crossing points between non-interacting potential energy surfaces, Theo. Chem. Acc. 99 (1998) 95–99.